Article

Layout Pattern of Small Panel and Large Coal Pillar for Rockburst Prevention and Water Control under Extra-Thick Water-Bearing Key Strata

Ning Zhang [1], Anye Cao [1,2,*], Weiwei Zhao [1], Qi Hao [1], Guowei Lv [1] and Baixuan Wu [1]

1   School of Mines, China University of Mining and Technology, Xuzhou 221116, China;
    ts21020069a31tm@cumt.edu.cn (N.Z.); ts21020074a31tm@cumt.edu.cn (W.Z.);
    tb21020009b0@cumt.edu.cn (Q.H.); tb22020052p41@cumt.edu.cn (G.L.); ts22020195p21@cumt.edu.cn (B.W.)
2   Jiangsu Engineering Laboratory of Mine Earthquake Monitoring and Prevention, China University of Mining
    and Technology, Xuzhou 221116, China
*   Correspondence: 4992@cumt.edu.cn

Abstract: There is a very thick water-bearing key strata above the coal seam in the Binchang mining area. When the mining scale is large, it easily breaks and leads to rockburst with a surge of water gushing in the panel. Adopting the layout pattern of a small panel and a large coal pillar can improve the stability of the main key strata, but at present, the research on the layout pattern of a small panel and a large coal pillar under extra-thick water-bearing key strata is still not perfect. Therefore, taking the second and third panels of a mine in Binchang as the engineering background, the width of the coal pillar and the mining scale of the panel are optimized by means of theoretical analysis, field measurement, and numerical simulation to prevent rockburst and control water inflow. The results show: (1) through theoretical calculation, it is deduced that the critical width of instability of the isolated coal pillar in the current mining scale is 257 m, and the critical mining scale of breaking and instability of the main key strata in the third panel is 537 m; (2) considering the bearing capacity of the isolated coal pillar and the recovery rate of coal resources, the reasonable width of the isolated coal pillar is 210~270 m, and when the width is 200 m and 250 m, the reasonable mining scale of the third panel is 490~550 m and 640~700 m, respectively; (3) the field practice shows that the actual width of the coal pillar between the second and third panels is less than the reasonable width, and the stress concentration in the isolated coal pillar area is relatively high, so the roof deep hole blasting and large-diameter drilling in coal seam are adopted to relieve pressure. After taking pressure relief measures, the stress concentration in the isolated coal pillar area is effectively reduced, and the pressure relief effect is remarkable.

Keywords: rockburst; extra thick; water-bearing key strata; width of panel-isolated coal pillar; mining scale of panel

1. Introduction

Rockburst is a phenomenon in coal mining where the coal rock mass suddenly fails, releasing a substantial amount of energy, which can lead to the deformation of the roadway surrounding the rock, equipment damage, and potential disasters such as coal and gas outburst and water inrush [1–8]. The Binchang mining area is one of the major Chinese coal-producing regions, which is generally faced with the situation that the mining depth is large and there is an extra-thick water-bearing sandstone layer above it. With the increase in the panel mining scale, the extra-thick water-bearing sandstone strata is broken and unstable, which leads to rockburst. At the same time, it is accompanied by a certain degree of water gushing [9–11]. Therefore, the adoption of the layout pattern of a small panel and a large coal pillar is of great significance to ensure the safe and efficient production of coal resources in the Binchang mining area.

The movement and rupture of the overlying strata is one of the crucial factors contributing to rockburst, and extensive research has been conducted by experts globally on the connection between overlying strata movement and rockburst. WANG Jiachen et al. put forward the masonry beam theory, gave the occlusal mode of broken rock mass and the mechanical conditions of instability, further developed the key layer theory, and explained the law of integral migration of overlying rock from the underground mining space to the surface [12]. Xu Xuefeng et al. studied the stress distribution characteristics of rocks surrounding the roadway under the super-thick conglomerate stratum. After the mining of several working faces, the extra-thick conglomerate has a large-scale hanging roof, resulting in an "O" type abutment pressure circle in the coal body around the goaf. The rockburst risk is high in the middle of the roadway [13]. Jiang Fuxing et al. investigated the impact of the overlying main key strata on the risk of rockburst in the mining face, and revealed the mechanism of rockburst induced by the breaking of super-thick main key strata [14]. Yang Weili et al. studied the impact mechanism of isolated island working faces under extra-thick magmatic rock, proposing criteria for judging the impact of isolated island working face under extra-thick magmatic rock instability [15]. Cao Anye et al. studied the effect of spatial structure and fracture migration characteristics of thick hard overburden on mine earthquake activity, and obtained the evolution characteristics of mine earthquake distribution in the process of mining in the isolated island working face [16]. Bai Xianqi et al. investigated the mechanism of thick overlying strata structure rupture inducing mine tremor events, proposing that the increase in goaf area causes vertical 'O-X' type fractures in the thick sandstone layer above the coal seam, triggering mine tremor events [17]. Zhai Minghua et al. studied the regularities of the dynamic impact induced by the movement of thick and hard strata, proposing that mining in critical working faces leads to the rupture of thick and hard strata, thereby inducing strong mine tremors or rockburst [18].

Regarding the mechanism of rockburst in the isolated coal pillar area, Wang Bo et al. studied the mechanism of rockburst in the isolated coal pillar area and developed a rational design method for the width of isolated coal pillars to control rockburst [19]. Xue Chengchun et al. investigated the mechanism of rockburst in irregular the isolated island coal pillar area, revealing that as the working face advances, the stress distribution inside the coal pillar shows an asymmetric 'saddle-shaped' pattern, and the stress peak continually increases, leading to coal pillar instability [20]. Feng Feilong et al. concluded that the transfer load of the overlying strata in the goaf increases the static load stress in the goaf side of the fully mechanized top coal caving pillar, which is superimposed with a hard roof breaking dynamic load to induce rockburst [21]. Li Dong et al. studied the mechanism of rockburst during the mining process of the working face with a large coal pillar on one side of the fold structure area [22]. Xu Xuhui et al. researched the mechanism of rockburst in the roadway under the disturbance of remaining coal pillars in large mining height mining faces, determining the reasonable layout positions for the roadway [23]. Zhang Shuai et al. optimized the pillar size of isolated island panel gob-side entry driving in deep inclined coal seams [24]. Li Xiaobin et al. studied the coal pillar width and surrounding rock control of gob-side entry in extra-thick coal seams [25]. Yang Kai et al. studied the reasonable width of coal pillars in high-strength mining roadways [26].

The mining depth of a mine in Binchang is nearly 1000 m, and the sandstone aquifer of the Luohe formation is overlying it. The inclined mining scale of the second panel of the mine is 900 m, which leads to the rockburst caused by the fracture and instability of the upper super-thick main key strata, accompanied by water inflow. To prevent rockburst and control water inflow, the third panel adopts the small panel and large coal pillar layout pattern. However, at present, there is limited research on the layout pattern of the panels beneath the thick water-bearing key strata. Therefore, through the methods of theoretical analysis, field measurement, and numerical simulation, from the stability of the isolated coal pillar and the main key strata above the goaf, this paper studies the overlying rock breaking rule and the stress evolution characteristics of the isolated coal pillar under the different layout pattern of a small panel and a large coal pillar, and optimizes the width

of the isolated coal pillar and the mining scale of the panel. It provides a reference for the prevention and control of rockburst in mines with similar conditions.

2. Engineering Background

2.1. Mining Geological Conditions

The mine is located in the northwest part of the Binchang mining area in Shanxi Province, with a depth of nearly one kilometer. It primarily extracts coal from the 4# coal seam, the dip angle of the 4# coal seam is 2°~11°, the average dip angle is 6.5°, and the 4# coal seam has strong bursting liability. The second panel is positioned to the east of the west-wing main roadway. The length on strike is approximately 1050–1450 m, the inclined width is about 900 m, and the area is about 1.35 km². The thickness of the 4# coal seam in the second panel is 0.8–15.7 m, with an average of 10.5 m, and the buried depth is 850 m to 1000 m. Five working faces are arranged in the second panel, each separated by small coal pillars measuring 5.0–7.0 m, and all adopting the fully mechanized top coal caving method. Among them, the mining height of LW205 is 3.5 m and the coal caving height is 5.5 m, which ends in September 2021. The third panel is arranged as a small-panel layout, situated to the northwest of the second panel. There is a panel isolation coal pillar with a width of 200 m between the second and third panels. The inclined width of the third panel is approximately 550 m. The layout of the second and third panels is illustrated in Figure 1.
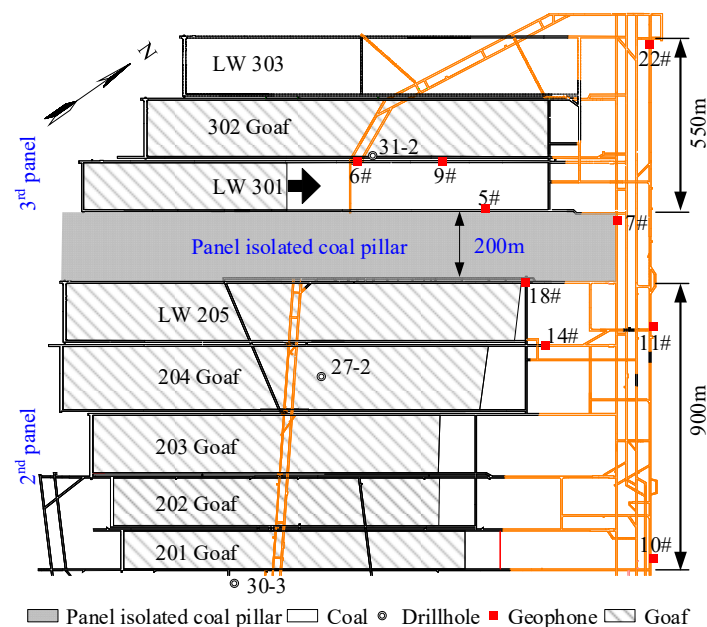

Figure 1. Schematic diagram of the working faces layout of the 2nd and 3rd panels.

According to the drilling holes 31-2, 27-2, and 30-3 near the second and third panels (see Figure 1 for the borehole locations), combined with the theory of key strata, the medium-coarse sand strata in the middle and upper part of the Luohe formation are the main key strata, with a thickness of 184–400 m and a distance of 113–294 m from the 4# coal seam. In the second panel, the thickness of the main key strata on the side of the 201 goaf is larger, while that on the side of working face 205 (LW205) is smaller. Additionally, based on in situ logging data, the water-rich aquifer is entirely present in the Luohe formation, with the middle section of the Luohe formation containing 75% of the water-rich aquifer. This aquifer has a thickness ranging from 90 to 110 m, its average porosity is 15.44%, its average unit water inflow is 1.305 to 2.248 L/(s·m), and the permeability coefficient of it is 0.06~1.552 m/d. It is recharged by the lateral runoff of groundwater, so it is difficult to drain [27]. The stratigraphic relationship between the water-rich aquifer and the main key strata is shown in Figure 2.
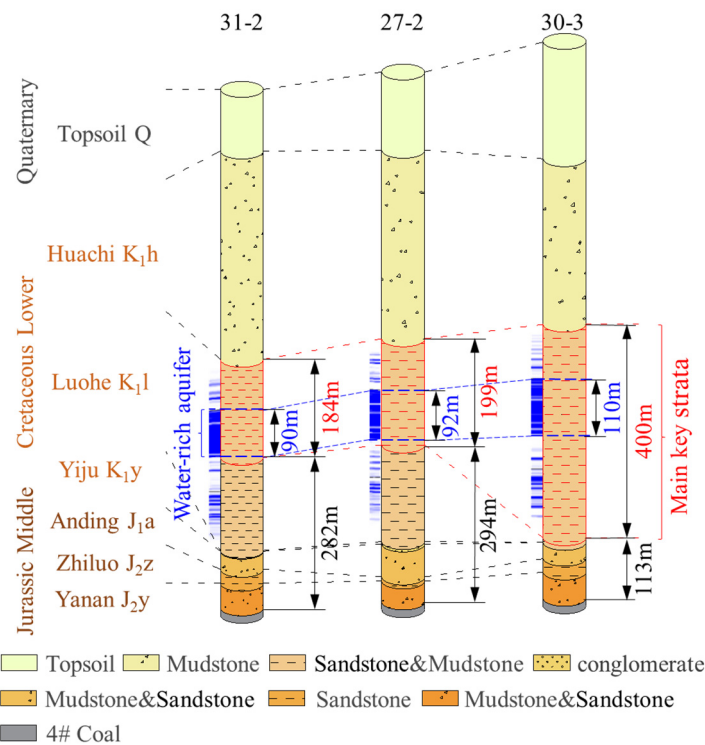
Figure 2. Schematic diagram of the stratigraphic structure in the 2nd and 3rd panels.

2.2. Analysis of the Spatial Distribution Characteristics of Large-Energy Microseismic Events and Water Inrush Situations

The second panel consists of five working faces, and the varying maximum water inflows of different working faces at the initial mining stage is illustrated in Figure 3. The maximum value of water inflow in the initial mining stage of different working faces has opposite characteristics with the corresponding mining distance. When mining to working face 202, the maximum value of water inflow increases slightly. As mining progresses to the working faces 203 and 204, it is basically stable, which is around 600–700 m^3/h. However, when mining reaches working face 205 (LW205), it sharply rises to 1500 m^3/h. In the initial mining stage of the working faces 202, 203, and 204, the water-conducting fractures develops to the lower part of the Luohe formation. At this point, the maximum water inflow in the initial mining stage of the three working faces is basically stable. However, in the mining of working face 205 (LW205), the water-conducting fractures from the working face extend to the lower part of the main key strata, which is in the middle part of the Luohe formation, communicating with a highly water-bearing layer. This leads to a sudden increase in the maximum water inflow in the initial mining stage of working face 205 (LW205). This shows that with the increase in the inclined mining scale, the development height of water-conducting fractures also increases, and the extra-thick key strata have a certain control effect on the overlying strata movement failure and the development of water-conducting fractures.

Figure 4 shows the large-energy (larger than 1×10^4 J) microseismic events location profile of working face 205 (LW205) from January 2020 to September 2021. The main key strata near the open-off cut of working face 205 (LW205) are higher, and along the mining direction of the working face, the thickness of the main key layer increases and the distance to the coal seam decreases. From January 2020 to September 2021 in working face 205, there are large-energy microseismic events in the main key strata above the coal seam, particularly in the middle part of the working face and on the side of the roadway for removing face. This indicates that with the increase in the inclined mining scale of the second panel, fractures develop into the thick main key strata, resulting in frequent

occurrences of large-energy microseismic events, and there is a risk of failure and instability in the extra-thick main key strata.
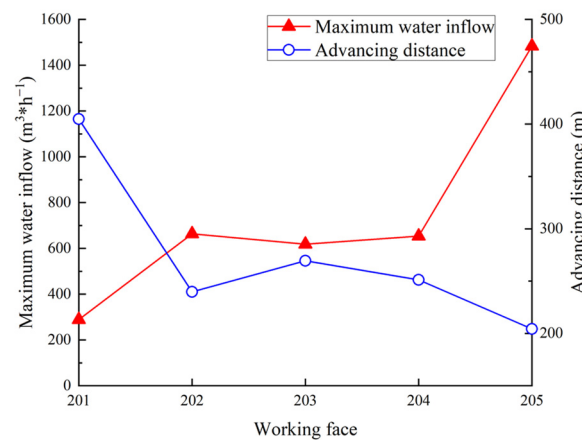

Figure 3. The maximum water inflow and corresponding advancing distance in initial mining stage of multi-working faces in the 2nd panel.
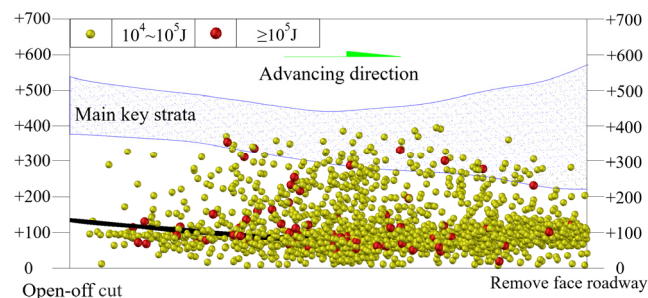

Figure 4. Positioning section of large-energy microseismic event of working face 205 (LW205).

Based on the spatial distribution of large-energy microseismic events and the water inflow situation in working face 205, it is evident that large-energy microseismic events have occurred in the main key strata, and the water inflow in working face 205 is substantial. This shows that after the mining of working face 205, the overlying strata above the coal seam are active violently, and the water-conducting fractures extend to the water-rich aquifer in the middle section of the Luohe formation. The main key strata above the second panel had reached their deflection limit, and there is a risk of breaking and destabilizing. In order to reduce the risk of rockburst and control water inflow, it is necessary to optimize the width of the isolated coal pillar and the mining scale of the panel, which can avoid the influence of rock stratum movement above the goaf in the second panel on the mining of the third panel. Therefore, it is necessary to make an in-depth study on the layout pattern of a small panel and a large coal pillar under the extra-thick water-bearing key strata, so as to provide theoretical support for rockburst prevention and water control under these kinds of geological conditions.

3. Theoretical Analysis of Rational Layout Pattern of Small Panel and Large Coal Pillar

Based on the key strata theory, the stability of the extra-thick sandstone key strata overlying the coal seam determines the characteristics of the movement and rupture of the overlying strata above the goaf, thereby influencing the stress distribution and stability of the coal pillar. According to the surface subsidence measurements in October 2021, the subsidence depth of the second panel is 637 mm, with a subsidence coefficient of 0.06. In the third panel, the subsidence depth is 233 mm, with a subsidence coefficient of 0.02. This indicates that the overlying strata have not fully subsided, and the extra-thick sandstone key strata have a certain flexural deformation, but still maintain relative stability.

With the increase in mining scale, there is a risk of coal pillar instability-induced rockburst and thick hard roof breakage-induced rockburst in the stope. Therefore, it is necessary to adopt the layout pattern of a small panel and a large coal pillar. Analyzing the stability of the panel-isolated coal pillar and the main key strata above the goaf, the critical width of the panel-isolated coal pillar and the critical mining scale of the small panel are determined.

3.1. Analysis of the Width of Panel Isolation Coal Pillar

The load borne by the isolated coal pillar comes from two sources. One is the self-weight of the overlying rock layer above the coal pillar, and the other is the transfer stress of the overlying rock layer on both sides of the goaf. Based on this, an analysis model for the force on the panel-isolated coal pillar is established, as shown in Figure 5. In Figure 5, L_1 represents the goaf width of the third panel, L_2 represents the goaf width of the second panel, D represents the width of the panel-isolated coal pillar, and H represents the burial depth of the two panels.
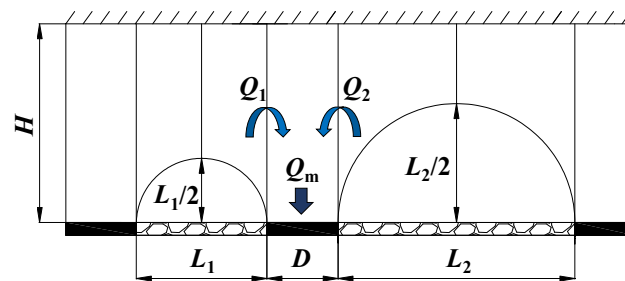

Figure 5. Stress analysis model of panel-isolated coal pillar.

From Figure 5, it can be observed that the load borne by the panel-isolated coal pillar Q_t includes the self-weight of the coal pillar Q_m, the load transmitted by the overlying rock layer of the goaf in the third panel Q_1, and the load transmitted by the overlying rock layer of the goaf in the second panel Q_2, namely

$$Q_t = Q_m + Q_1 + Q_2 \tag{1}$$

Based on the geometric relationship, Q_t, Q_1, and Q_2 can be expressed as follows:

$$Q_m = \gamma H D \tag{2}$$

$$Q_1 = \frac{\gamma}{2}\left(HL_1 - \frac{\pi L_1{}^2}{8}\right) \tag{3}$$

$$Q_2 = \frac{\gamma}{2}\left(HL_2 - \frac{\pi L_2{}^2}{8}\right) \tag{4}$$

In the equation, γ represents the bulk density of overlying rock strata.

As shown in Figure 6, in the layout pattern of a small panel and a large coal pillar, the stress distribution in the elastic area of the panel-isolated coal pillar is uniform. When the bearing stress of the panel-isolated coal pillar approaches bearing capacity, the coal pillars tend to reach a critical state of high stress instability. Under mining disturbance, this can easily induce rockburst. The calculation of the bearing stress in the elastic zone of the panel-isolated coal pillars is as follows:
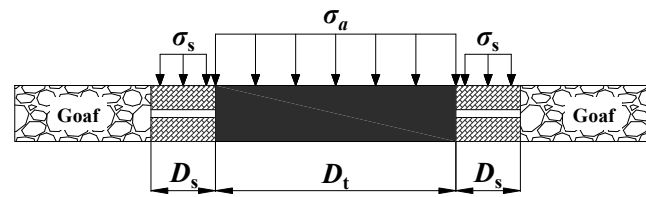
$$\sigma_a = \frac{Q_t - 2Q_s\sigma_s}{D_t} \tag{5}$$

Figure 6. Analysis model of bearing stress in elastic zone of panel-isolated coal pillar.

In the equation, σ_a represents the bearing stress in the elastic area; D_t represents the width of the elastic area, $D_t = D - 2D_s$; D_s represents the width of the plastic area; σ_s represents the bearing stress in the plastic area, which is equal to the uniaxial compressive strength of coal.

The ratio of the bearing stress in the elastic area of the panel-isolated coal pillar to its bearing capacity is given by:

$$\mu = \frac{\sigma_a}{\sigma_{3c}} \tag{6}$$

In the equation, σ_{3c} represents the bearing capacity of the coal, taken as three times the uniaxial compressive strength of coal.

Based on the actual conditions of the mine, $\gamma = 25$ kN/m³, $H = 950$ m, $L_1 = 550$ m, $L_2 = 900$ m, $D = 200$ m, $D_s = 20$ m, the uniaxial compressive strength of coal $\sigma_c = 18$ MPa. Substituting these parameters into Equations (1) to (6), $\mu = 1.77 > 1$. If $\mu = 1$, $D = 257$ m can be obtained under the condition that the inclined width of the goaf on both sides of the panel-isolated coal pillar is constant. Therefore, under the current layout pattern, there is a risk of rockburst induced by instability of the panel-isolated coal pillar, and the critical width of instability is 257 m.

3.2. Analysis of Mining Scale in Panel

Under the action of the self-weight of the overlying rock strata and the stress transmitted from the overlying rock strata to both sides of the goaf, the panel-isolated coal pillar is compressed. The main key strata were flexed under the load of the overlying strata. As the scale of the goaf on both sides of the panel-isolated coal pillar increases, the transmitted stress from the goaf on both sides also increases, leading to an increase in the compression of the panel-isolated coal pillar. When the compression of the coal pillar exceeds the deflection limit of the main key strata, the main key strata and the lower strata are separated. At this point, the central part of the main key strata is unsupported, and the thick hard sandstone main key layer is prone to fracturing, triggering large-energy microseismic events and rockburst.

Based on the mechanical characteristics of the key strata, the main key strata after delamination from the lower rock strata can be considered as a suspended beam fixed at both ends. The stress from the overlying rock layer can be simplified as a uniformly distributed load, with a concentrated reaction force acting on both sides of the beam. Taking the center of the left end of the suspended beam as the origin, the direction along the axis of the suspended beam as the x-axis, and the direction along the thickness of the suspended beam as the y-axis, an analysis model of the flexural deformation of the main key strata is established, as shown in Figure 7.

In Figure 7, q_0 is the uniformly distributed load of the overlying rock above the main key strata (including the self-weight of the main key strata), h is the thickness of the main key strata, l_1 is the width of the third panel, l_2 is the width of the second panel, d is the width of the panel-isolated coal pillar, F is the reaction force at the fixed support end of the main key strata, and M is the bending moment at the fixed support ends of the main key strata. The ultimate span l of the key strata can be expressed as follows:

$$l = h\sqrt{\frac{\delta}{q_0} + 1 + \frac{5}{4}\mu} \tag{7}$$

In the equation, δ is the uniaxial tensile strength of the main key strata, μ is the Poisson's ratio of the main key strata.
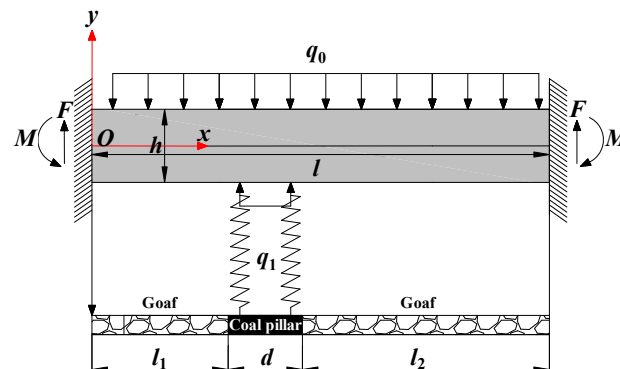

Figure 7. Deflection deformation analysis model of the main key strata.

Simultaneously, after the separation of the main key strata and the lower rock layer, the deflection equation of the beam axis is given by:

$$z = \frac{q_0 x^3}{2Eh^3}(2l + x) \tag{8}$$

Under the condition of fixed support at both ends, the maximum deflection occurs at the midpoint of the beam, that is, $x = l/2$. Therefore, the maximum deflection of the beam is given by:

$$\omega_{max} = z_{(x=l/2)} = \frac{5q_0 l^4}{32Eh^3} \tag{9}$$

Before mining the second and third panels, the panel-isolated coal pillar was only affected by the original overlying rock stress. Based on the stress analysis model of the coal pillar in Figure 4, the compression amount v of the isolated coal pillar during mining can be calculated as follows:

$$v = \varepsilon m = \frac{Q_t - Q_0}{E_0 d_0} m \tag{10}$$

In the equations, m represents the mining height, ε represents the strain of the isolated coal pillar, E_0 is the elastic modulus of the coal, d_0 is the elastic area width of the panel-isolated coal pillar.

According to the actual conditions of the mine, $h = 200$ m, $\delta = 2.01$ MPa, $\mu = 0.24$, $E = 8 \times 10^3$ MPa, $E_0 = 2.67 \times 10^3$ MPa, $d_0 = 160$ m, the uniformly distributed load above the key strata $q_0 = 12.50$ MPa. Substituting these values into the calculations, the limit span l of the key strata is determined to be 241 m, which is greater than D. The maximum deflection of the main key layer ω_{max} is 0.104, before mining in the second and third panels, the initial load on the isolated coal pillar $Q_0 = \gamma H d$. The compression amount of the isolated coal pillar $v = 0.247$. If $v = \omega_{max}$, keeping the width of the panel-isolated coal pillar and the mining scale of the second panel unchanged, $l_1 = 537$ m is calculated. Therefore, in the current layout pattern of a small panel and a large coal pillar, the compression amount of the isolated coal pillar is greater than the limit deflection of the main key strata. There is a risk of breaking and instability in the extra thick key strata, inducing the danger of rockburst. The critical mining scale for the small panel is determined to be 537 m.

4. Study on Mining Layout Pattern Based on Numerical Simulation

Through the finite element numerical simulation software FLAC3D 6.00.69, we investigate the stress and elastic strain energy distribution and evolution pattern of panel-isolated coal pillars under various isolation pillar widths and different small panel mining scales.

The analysis aims to analyze the stability of panel-isolated coal pillars, ultimately determining a reasonable width for the isolation coal pillar and the small panel mining scale.

4.1. Establishment of Numerical Model and Design of Simulation Scheme

Based on the geological conditions and mining layout of the second and third panels of the mine, a numerical simulation computational model is established for the layout pattern of a small panel and a large coal pillar beneath the extra-thick water-bearing key strata. The size of the numerical simulation model is 4300 m × 3300 m × 1280 m, and the model is divided into 2,898,252 zones. The model employs the Mohr–Coulomb constitutive model, fixes the bottom boundary of the model, applies a displacement constraint to the surrounding boundaries, and has a free boundary at the top, with the top representing the ground surface. Combining with field measurement and the rock mechanics test, the rock's physical and mechanical parameters used in the model are listed in Table 1. The schematic diagram of the model is shown in Figure 8.

Table 1. Physical and mechanical parameters of model.

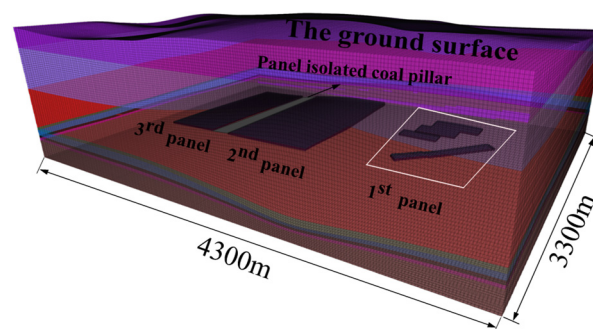| Lithology	Density (kg/m^3)	Bulk Modulus (GPa)	Shear Modulus (GPa)	Friction Angle (°)	Cohesion (MPa)
Loess	1640	2.21	0.37	25	0.01
Sandy mudstone	2480	1.13	0.67	39	2.92
Medium grain sandstone	2400	7.32	4.57	41	1.91
Coarse grain sandstone	2510	9.68	6.37	41	2.32
Coal seam	1400	3.49	2.01	36	1.18
Mudstone	2550	0.98	0.70	37	2.61

Figure 8. Numerical model of panel excavation.

The orthogonal experimental method is employed to investigate the influence of the width of the panel-isolated coal pillar and the mining scale of the small panel on the stability of the panel-isolated coal pillar. The width of the panel-isolated coal pillar is varied from 150 m to 300 m. When the width of the panel-isolated coal pillar is 200 m, the mining scale of the third panel is set between 400 m and 580 m. Similarly, when the width of the panel-isolated coal pillar is 250 m, the mining scale of the third panel ranges from 580 m to 760 m. The interval between values is set at 30 m.

4.2. Effect of Coal Pillar Width on Stability of Panel-Isolated Coal Pillar

Under the condition of different widths of the panel-isolated coal pillar, the vertical stress tendency slice contour and elastic strain energy plane distribution contour of the panel-isolated coal pillar area after excavation in the second and third panels are shown in Figures 9 and 10. When the width of the panel-isolated coal pillar is less than 200 m, there is a higher degree of stress concentration and energy accumulation in the panel-isolated coal pillar area. When the coal pillar width exceeds 210 m, the stress and energy accumulation in the panel isolated coal pillar area are higher only near the areas adjacent to the two sides

of the goaf, while the stress concentration and energy accumulation in the elastic core zone of the isolation coal pillar are relatively low.
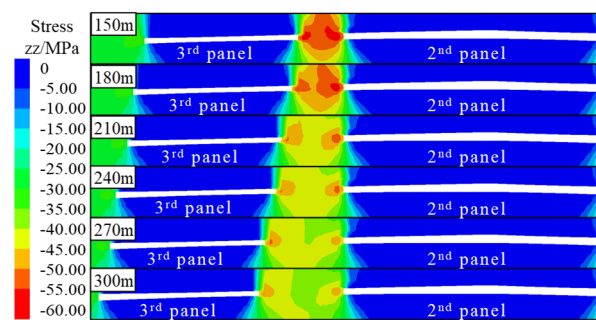

Figure 9. Vertical stress tendency slice contour of panel-isolated coal pillar with different widths.
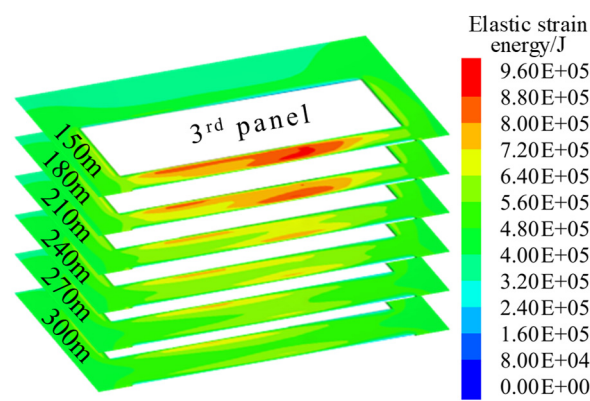

Figure 10. Plane distribution contour of elastic strain energy in the panel-isolated coal pillar with different widths.

The variation curve of stress along the inclination of the panel-isolated coal pillar is shown in Figure 11. With the increase in the width of the panel-isolated coal pillar, the degree of stress concentration in the panel-isolated coal pillar weakens. The stress peak decreases from 57.34 MPa to 49.20 Mpa, and the stress concentration factor decreases from 2.07 to 2.41. When the width of the panel-isolated coal pillars is 150 m and 180 m, the stress peaks are 57.34 MPa and 55.80 MPa, respectively, both exceeding the uniaxial compressive strength of three times the coal, which is 54 MPa. At this point, the panel-isolated coal pillar is in a critical and unstable state.
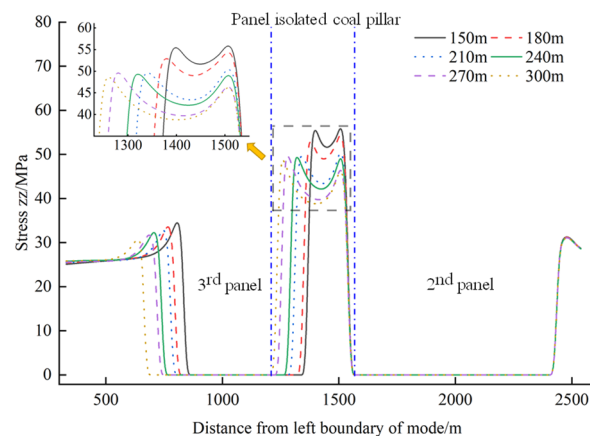

Figure 11. Vertical stress variation curve of the panel-isolated coal pillar area under different widths of the panel-isolated coal pillar.

The analysis of the above simulation results shows that under the condition that the goaf area on both sides of the panel-isolated coal pillar is unchanged, the stress transferred from the goaf on both sides of the panel-isolated coal pillar remains unchanged, but the width of the panel-isolated coal pillar increases, leading to a gradual reduction in stress concentration and energy accumulation in the panel-isolated coal pillar area. Considering the stability of the panel-isolated coal pillar and resource recovery rate, combined with the simulation results mentioned above, under the current small panel mining scale of 550 m, the reasonable range for the width of the panel-isolated coal pillar is 210 m to 270 m, and the mining district recovery ratio is between 75% and 77%.

4.3. Influence of Panel Mining Scale on the Stability of Panel-Isolated Coal Pillar

When the width of the panel-isolated coal pillar is 200 m and 250 m, the vertical stress tendency slice contour and elastic strain energy plane distribution contour of the panel-isolated coal pillar area after excavation in the second and third panels under different panel mining scales are shown in Figures 12 and 13. With the increase in the mining scale in the third panel, the degree of stress concentration and energy accumulation in the panel-isolated coal pillar area intensifies. Under the condition of a 200 m-wide panel-isolated coal pillar, when the mining scale in the third panel is less than 400 m, the degree of stress concentration and elastic strain energy accumulation in the panel-isolated coal pillar area is relatively low. There is only a stress concentration area near the goaf on both sides. When the mining scale in the third panel exceeds 520 m, the degree of stress concentration and elastic strain energy accumulation in the elastic core area in the middle of the isolated coal pillar area becomes higher, and the stress concentration area gradually develops to the top of the coal seam. Under the condition of a 250 m-wide panel-isolated coal pillar, when the mining scale in the third panel reaches 700 m and 730 m, the stress and energy accumulation area gradually evolve towards the elastic core area in the middle of the coal pillar. When the mining scale in the third panel reaches 760 m, the degree of stress concentration and elastic strain energy accumulation in the elastic core area in the middle of the panel-isolated coal pillar area becomes higher, and a stress concentration area appears in the roof rock layer.
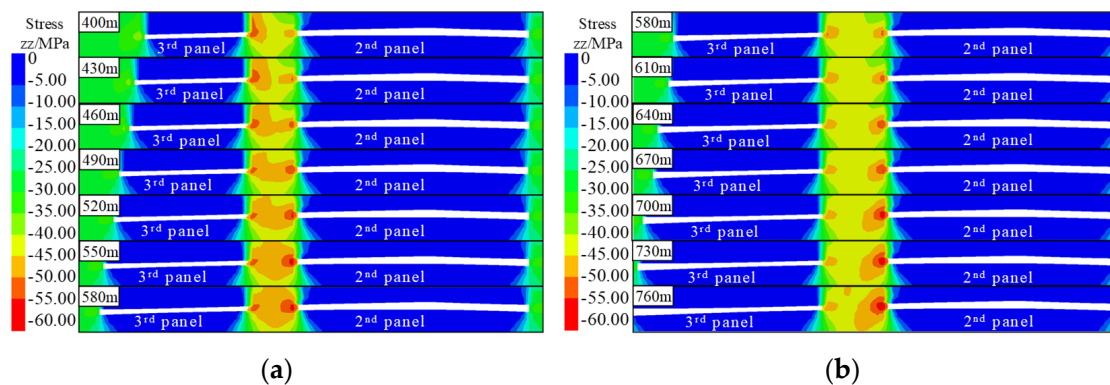

Figure 12. Slice contour of vertical stress tendency in the panel-isolated coal pillar area under different mining scales of panel. (**a**) 200 m-wide panel-isolated coal pillar. (**b**) 250 m-wide panel-isolated coal pillar.

Draw the stress variation curve along the inclination of the isolated coal pillar area under different panel mining scale, as shown in Figure 14. With the increase in the panel mining scale, the degree of stress concentration in the panel-isolated coal pillar area increases. Under the condition of a 200 m-wide panel-isolated coal pillar, the stress peak increases from 51.55 MPa to 54.98 MPa, and the stress concentration factor increases from 2.17 to 2.31. When the width of the mining scale of the panel is 550 m, the vertical stress peak in the panel-isolated coal pillar area is 54.08 MPa, exceeding the uniaxial compressive strength of three times the coal, which is 54 MPa. At this point, the isolated coal pillar in the panel area was in a critical and unstable state. Under the condition of a 250 m-wide

isolated coal pillar, the stress peak increases from 49.78 MPa to 55.83 MPa, and the stress concentration factor increases from 2.10 to 2.35. When the width of the mining scale of the panel is 700 m, the vertical stress peak in the panel-isolated coal pillar area is 54.75 MPa, exceeding the uniaxial compressive strength of three times the coal, which is 54 MPa. At this point, the panel-isolated coal pillar was in a critical and unstable state.
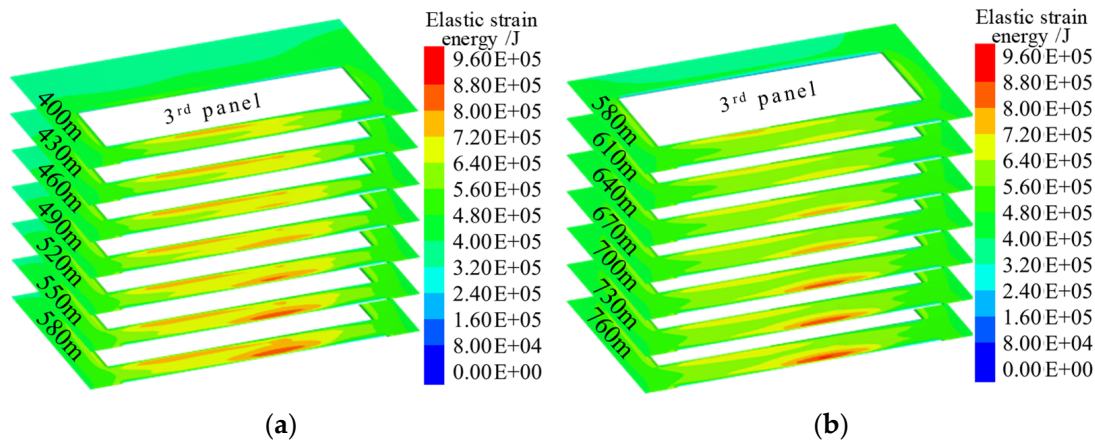

(a)   **(b)**

Figure 13. Plane distribution contour of elastic strain energy in the panel-isolated coal pillar under different mining scales of panel. (**a**) 200 m-wide panel-isolated coal pillar. (**b**) 250 m-wide panel-isolated coal pillar.

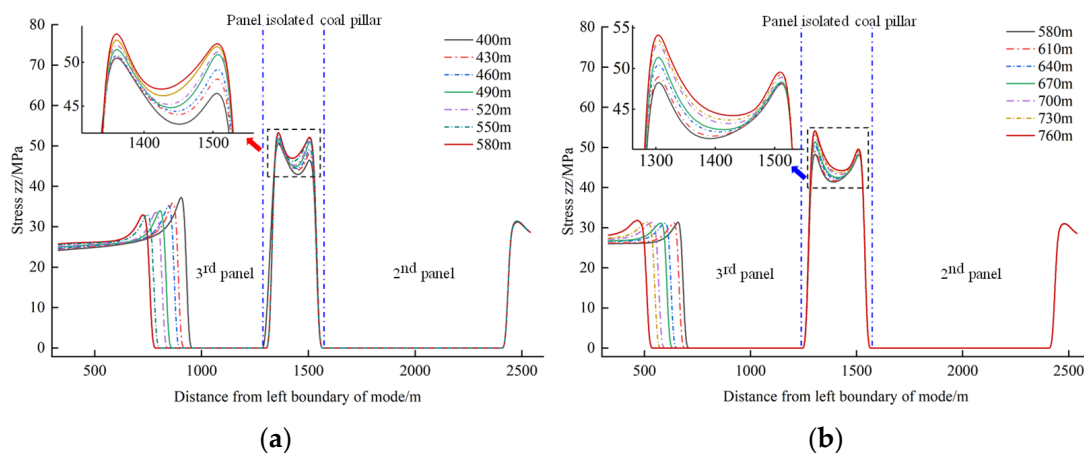**(a)**   **(b)**

Figure 14. Vertical stress variation curve of the panel-isolated coal pillar area under different mining scales of panel. (**a**) 200 m-wide panel-isolated coal pillar. (**b**) 250 m-wide panel-isolated coal pillar.

Analyzing the above simulation results reveals that with the increase in the mining scale of the small panel, the transferred stress from the goaf on both sides of the panel-isolated coal pillar increases. However, with the width of the panel-isolated coal pillar remaining unchanged, the average bearing stress of the coal pillar increases, leading to the panel-isolated coal pillar approaching a critical state of instability. Considering the stability of the panel-isolated coal pillar and the resource recovery rate, combined with the simulation results mentioned above, under the condition of a 200 m-wide panel-isolated coal pillar, the reasonable mining scale for the small panel is between 490 m and 550 m, and the mining district recovery ratio is between 75% and 78%. Under the condition of a 250 m-wide panel-isolated coal pillar, the reasonable mining scale for the small panel is between 640 m and 700 m, and the mining district recovery ratio is between 78% and 79%.

5. Engineering Practice of Pressure Relief and Rockburst Prevention Measures under the Layout Pattern of Small Panel and Large Coal Pillar

5.1. Control Effect of Rockburst under the Layout Pattern of Small Panel and Large Coal Pillar

After adopting the layout pattern of a small panel and a large coal pillar, the inclined mining scale of the third panel is 550 m, and the panel-isolated coal pillar's width is 200 m between the second and third panels, as shown in Figure 1. According to theoretical analysis and numerical simulation conclusions, under the current panel mining scale, the reasonable width for the panel-isolated coal pillar should be between 210 m and 270 m. The actual width of the coal pillar left between the second and third panels is less than the reasonable width, leading to a higher degree of stress concentration in the panel-isolated coal pillar area, posing a risk of rockburst during the mining process in the third panel. Based on the distribution characteristics of microseismic events greater than 1×10^3 J in the panel-isolated coal pillar area between the second and third panels during the monitoring period from September to December 2021, the plane distribution map of microseismic events in the isolated coal pillar area is shown in Figure 15. By December 2021, working face 205 (LW205) had completed mining, and working face 301 (LW301) had advanced 852 m, in the later stages of mining. During this stage, there were a lot of microseismic events on the side of the isolated coal pillar near working face 301 (LW301), and there were large-energy microseismic events in the elastic region of the coal pillar.
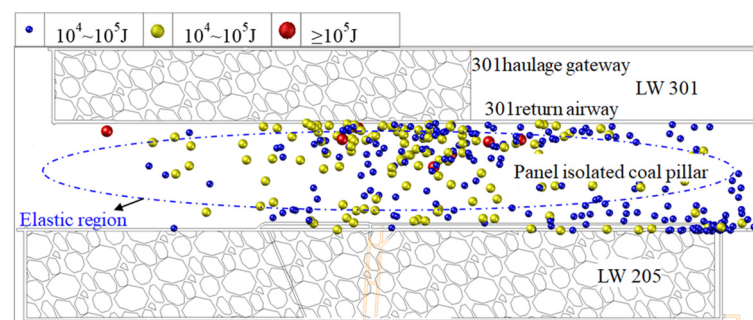

Figure 15. Plane distribution of microseismic events in the panel-isolated coal pillar area.

This indicates that with the advancement of working face 301, the goaf area in the third panel expands, and the stress on the panel-isolated coal pillar area increases. Combined with the mining disturbance to the panel-isolated coal pillar, there were many large-energy microseismic events in the panel-isolated coal pillar area, extending into the central elastic area. Therefore, under the current layout pattern of a small panel and a large coal pillar, the isolation protection effect of the panel-isolated coal pillars is limited, and there is still a certain risk of rockburst. Appropriate unloading and prevention of rockburst measures need to be taken.

5.2. Unloading and Prevention of Rockburst Measures

In response to the limited isolation effect of the panel-isolated coal pillar in the current layout pattern of a small panel and a large coal pillar, unloading and prevention of rockburst measures are implemented in the return airway of working face 301 (LW301) in the third panel. The pressure relief is carried out by roof deep hole blasting and large-diameter drilling in the return airway of working face 301 (LW301). The roof deep hole blasting can destroy the structural integrity of the roof above the return airway along the trough side of working face 301 (LW301), preventing the occurrence of large area roof suspension and reducing the lateral abutment pressure exerted on the panel-isolated coal pillar by working face 301 (LW301). The large-diameter drilling in the coal seam causes the coal on both sides of the return airway to break, transferring stress to the deeper part of the surrounding rock of the roadway, reducing the stress concentration in the panel-isolated coal pillar area, ultimately improving the stability of the panel-isolated coal pillar, and further reducing the risk of rockburst [28].

Two blasting hole schemes are used for unloading in the roof above the return airway in working face 301 (LW301): a fan-shaped roof hole in the working face and a down-groove cutting roof hole. For the fan-shaped hole blasting in the working face, a set of three holes (1#, 2#, 3#) is arranged, with hole positions at the shoulder recess on the production side; the distance between blasting holes is 15 or 20 m, the hole diameter is 85 mm, and the sealing length is not less than 15 m. For the cutting roof hole along the groove, a set of two holes (4#, 5#) is arranged; the opening position is the middle part of the roadway roof, the distance between the blasting holes is 5 m, the hole diameter is 85 mm, and the sealing length is not less than 15 m [29]. The specific blasting parameters are shown in Table 2 and Figure 16.

Table 2. Roof deep hole blasting parameters.

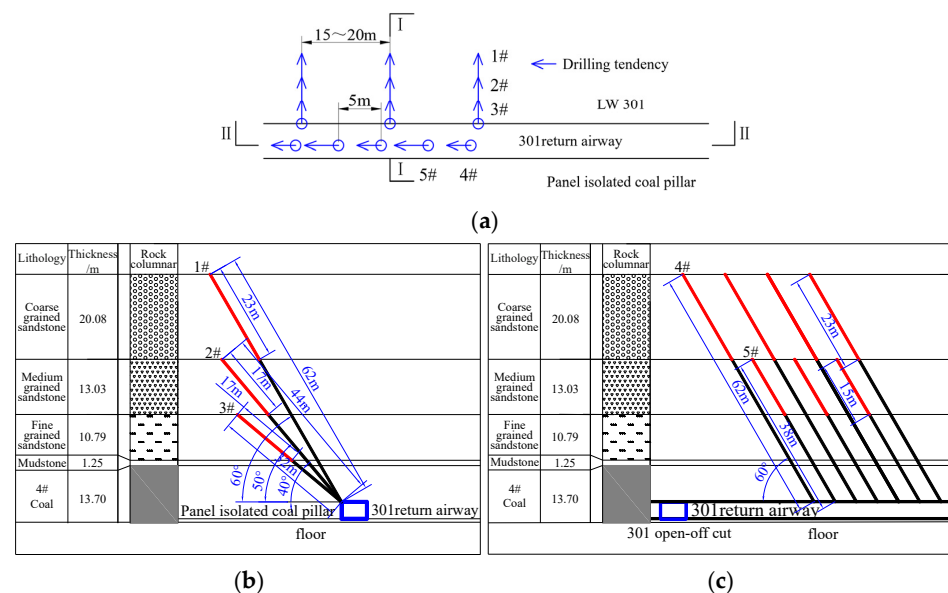| Drilling Number	Drilling Elevation Angle/(°)	Blast Hole Depth/m	Explosive Dosage/kg	End Hole Position
1#	60	62	60	Coarse grain sandstone
2#	50	44	40	Medium grain sandstone
3#	40	32	40	Fine grain sandstone
4#	60	62	60	Coarse grain sandstone
5#	60	38	40	Medium grain sandstone

Figure 16. Schematic diagram of the layout of the roof deep hole blasting. (**a**) Drill hole layout plan. (**b**) Schematic diagram of I-I section. (**c**) Schematic diagram of II-II section.

Large-diameter drilling is arranged in the vertical side of the LW301 return airway, with a hole depth of 30 m, a hole diameter of 150 mm, a sealing length of 3 m, and a hole spacing of 1 m or 2 m, with a distance of 1.2–1.5 m from the floor [30]. The layout of large-diameter coal seam drilling is shown in Figure 17.
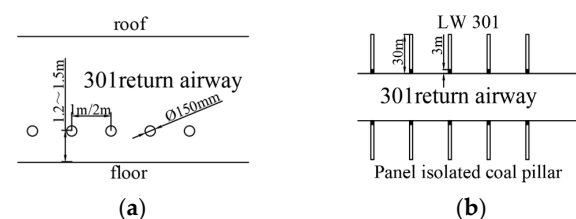

Figure 17. Schematic diagram of the layout of the large-diameter drilling in the coal seam. (**a**) Section diagram. (**b**) Plane diagram.

5.3. Unloading and Prevention of Rockburst Effect

Based on the microseismic events in the panel-isolated coal pillar area of the mine from August to October 2021, the seismic wave CT inversion was conducted. Through the inversion of seismic wave CT, the propagation velocity of the seismic wave in the coal rock mass can be obtained. The higher the velocity of the seismic wave in the coal rock mass, the higher the stress concentration degree [31,32].

Figure 18 shows the CT inversion contour of the panel-isolated coal pillar and its vicinity before and after pressure relief. On 15 September 2021, near the 120 m advance drainage roadway of the return airway in front of working face 301 (LW301), the positive anomaly coefficient of the wave velocity (An) was between 0.15 and 0.35, and there was a phenomenon of stress concentration. Before 18 October 2021, pressure relief measures such as deep borehole blasting in the roof and large-diameter drilling in the coal seam were implemented in this area and its vicinity. The CT inversion results on October 18 showed that the value of An in this area decreased significantly. On 4 November 2021, in the 200 m range of the advance drainage roadway of the return airway in front of working face 301 (LW301), the value of An was between 0.15 and 0.45, indicating stress concentration. Before November 16, appropriate pressure relief measures were taken in the corresponding region and its vicinity. The CT inversion results on November 16 showed a significant decrease in the anomaly coefficient of the wave velocity in the corresponding region. To sum up, after implementing deep borehole blasting and large-diameter drilling in the coal seam for unloading in the return airway in front of working face 301 (LW301), the stress concentration level in the panel-isolated coal pillar area was effectively reduced, demonstrating good unloading and an anti-burst effect.
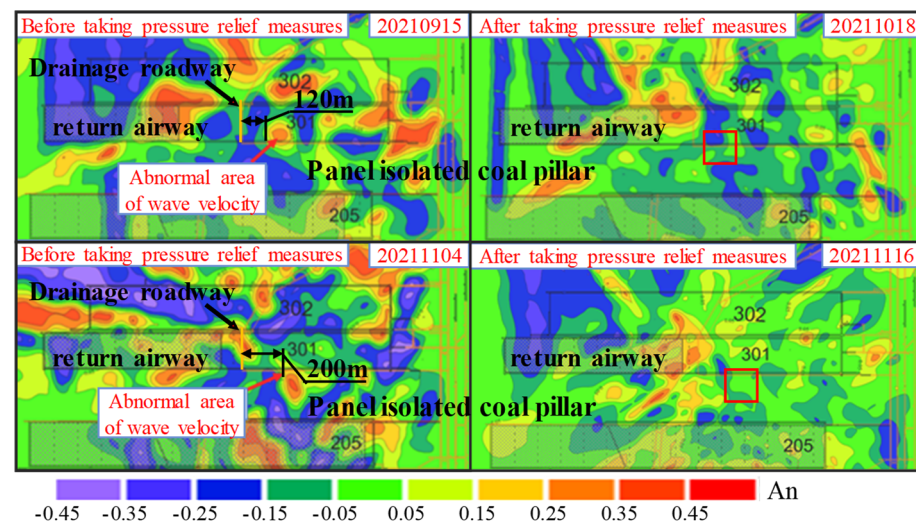

Figure 18. CT inversion contour of the panel-isolated coal pillar and its vicinity.

6. Conclusions

In this work, the reasonable range of the coal pillar width and mining scale of the panel are studied by means of theoretical analysis, field measurement, and numerical simulation. According to the achieved results:

(1) Based on the mechanical theory, considering the stability of the panel-isolated coal pillar and the main key strata above the goaf, it is derived that under the current mining layout, the critical width for the instability of the panel-isolated coal pillar is 257 m, and the critical mining width for the small panel is 537 m.

(2) With the increase in the width of the panel-isolated coal pillar and the decrease in the mining scale of the small panel, the stress concentration and energy accumulation in the panel-isolated coal pillar area decrease, enhancing the stability of the isolation coal pillar. Considering the stability of the panel-isolated coal pillar and the recovery

rate of coal resources, the reasonable range of the panel-isolated coal pillar is 210 m to 270 m. For a 200 m-wide panel-isolated coal pillar, the reasonable mining scale for the small panel is 490 m to 550 m; for a 250 m-wide panel-isolated coal pillar, the reasonable mining scale for the small panel is 640 m to 700 m.

(3) Practical mining experience indicates that despite adopting the small panel and large coal pillar layout pattern, the actual width of the coal pillar is less than the reasonable width, resulting in a higher degree of stress concentration in the panel-isolated coal pillar area and frequent large-energy microseismic events. Therefore, in the return airway of working face 301, deep borehole blasting and large-diameter drilling in the coal seam are employed for pressure relief. After implementing pressure relief measures, the CT inversion results in the panel-isolated coal pillar area show a significant reduction in the abnormal coefficient of wave velocity, indicating a notable pressure relief effect.

The key findings indicate that optimizing the dimensions of the longwall panel and coal pillar can ensure the stability of the extra-thick water-bearing key strata, reduce the stress concentration around the stope, and realize the purpose of rockburst prevention and water control. Further, the development law of the overlying rock fracture zone above the stope under different layouts can be studied to control the development height of the water-conducting fracture zone.

Institutional Review Board Statement: Not applicable.

Informed Consent Statement: Not applicable.

Data Availability Statement: The data used to support the findings of this study are available from the corresponding author upon request.

Conflicts of Interest: The authors declare no conflicts of interest.

References

1. Pan, Y.S.; Song, Y.M.; Liu, J. Pattern, change and new situation of coal mine rockburst prevention and control in China. *Chin. J. Rock Mech. Eng.* **2023**, *42*, 2081–2095.
2. Dou, L.M.; Tian, X.Y.; Cao, A.Y.; Gong, S.Y.; He, H.; He, J.; Cai, W.; Li, X.W. Present situation and problems of coal mine rock burst prevention and control in China. *J. China Coal Soc.* **2022**, *47*, 152–171.
3. Cao, A.Y.; Dou, L.M.; Bai, X.Q.; Liu, Y.Q.; Yang, K.; Li, J.Z.; Wang, C.B. State-of-the-art occurrence mechanism and hazard control of mining tremors and their challenges in Chinese coal mines. *J. China Coal Soc.* **2023**, *48*, 1894–1918.
4. Qi, Q.X.; Li, Y.Z.; Zhao, S.K.; Zhang, N.B.; Zheng, W.Y.; Li, H.T.; Li, H.Y. Seventy years development of coal mine rock burst in China: Establishment and consideration of theory and technology system. *J. Coal Sci. Technol.* **2019**, *47*, 1–40. (In Chinese)
5. Yuan, L. Control of coal and gas outbursts in Huainan mines in China: A review. *J. Rock Mech. Geotech. Eng.* **2016**, *8*, 559–567. [CrossRef]
6. Nguyen, P.M.V.; Litwa, P.; Przybylski, M. Field testing of the methods for prevention and control of coal and gas outburst—A case study in Poland. *Arch. Min. Sci.* **2023**, *68*, 639–654. [CrossRef]
7. Xu, T.; Tang, C.A.; Yang, T.H.; Zhu, W.C.; Liu, J. Numerical investigation of coal and gas outbursts in underground collieries. *Int. J. Rock Mech. Min. Sci.* **2006**, *43*, 905–919. [CrossRef]

8.   Jiang, Y.D.; Zhao, Y.X. State of the art: Investigation on mechanism, forecast and control of coal bumps in China. *J. Rock Mech. Eng.* **2015**, *34*, 2188–2204.

9.   He, J.; Dou, L.M.; Wang, S.W.; Shan, C.H. Study on mechanism and types of hard roof inducing rock burst. *J. Min. Saf. Eng.* **2017**, *34*, 1122–1127.

10.   Wang, H.W.; Deng, D.X.; Jiang, Y.D.; Shi, R.M.; Yang, G.Z.; Zahng, X.H. Study on the dynamic evolution characteristics of deformation and collapse of the extra-thick hard roof. *J. Min. Sci. Technol.* **2021**, *6*, 548–557.

11.   Junker, M. *Strata Control in In-Seam Roadways*; VGE Verlag: Berlin, Germany, 2009.

12.   Wang, J.; Xu, J.; Yang, S.; Wang, Z. Development of strata movement and its control in underground mining: In memory of 40 years of Voussoir Beam Theory proposed by Academician Minggao Qian. *J. Coal Sci. Technol.* **2023**, *51*, 80–94.

13.   Xu, X.F.; Dou, L.M.; Cao, A.Y.; Jiang, H.; Zhang, M.W.; Lu, Z.Y. Effect of overlying strata structures on rock burst and micro-seismic monitoring analysis. *J. Min. Saf. Eng.* **2011**, *28*, 11–15.

14.   Jiang, F.X.; Wei, Q.D.; Wang, C.W.; Yao, S.L.; Zhang, Y.; Han, R.J.; Wei, X.Z.; Li, Z.C. Analysis of rock burst mechanism in extra-thick coal seam controlled by huge thick conglomerate and thrust fault. *J. China Coal Soc.* **2014**, *39*, 1191–1196.

15.   Yang, W.; Jiang, F.; Yang, P.; Zhai, M.; Wang, Y.; Liu, W.; Zhang, J. Prevention of rockburst in large island longwall panels induced by instability of super-thick magmatic strata. *J. Rock Mech. Eng.* **2017**, *36*, 3382–3391.

16.   Cao, A.Y.; Dou, L.M.; Wang, C.B.; Yao, X.X.; Dong, J.Y.; Gu, Y. Microseismic Precursory Characteristics of Rock Burst Hazard in Mining Areas Near a Large Residual Coal Pillar: A Case Study from Xuzhuang Coal Mine, Xuzhou, China. *J. Rock Mech. Rock Eng.* **2016**, *49*, 4407–4422. [CrossRef]

17.   Bai, X.; Cao, A.; Yang, Y.; Wang, C.; Liu, Y.; Zhao, Y.; Guo, W.; Gu, Y.; Wu, Z. Study on movement law of extremely thick strata and triggering mechanism of mine earthquakes. *J. Coal Sci. Technol.* **2023**, *51*, 10–20.

18.   Zhai, M.; Jiang, F.; Zhu, S.; Zhang, M.; Yao, S.; Guo, X.; Sun, X. Research and application of mining design based on prevention of rock burst under giant thickness hard strata. *J. China Coal Soc.* **2019**, *44*, 1707–1715.

19.   Wang, B.; Zhu, S.; Jiang, F.; Liu, J.; Shang, X.; Zhang, X. Investigating the Width of Isolated Coal Pillars in Deep Hard-Strata Mines for Prevention of Mine Seismicity and Rockburst. *J. Energ.* **2020**, *13*, 4293. [CrossRef]

20.   Xue, C.; Cao, A.; Niu, F.; Wang, X.; Shen, Z.; Tang, K. Mechanism and prevention of rock burst in deep irregular isolated coal pillar. *J. Min. Saf. Eng.* **2021**, *38*, 479–486.

21.   Feng, L.; Dou, L.; Wang, H.; Wang, X.; Xu, G.; Zhang, Q.; Jiao, B. Mechanism of rockburst in dense roadway area near the goaf of fully-mechanized large pillars. *J. Min. Saf. Eng.* **2021**, *38*, 1100–1110+1121.

22.   Li, D.; Shi, X.; Zhao, C.; Ge, D.; Chen, Y.; Dong, C.; Jiang, F.; Wen, Z. Mechanism of rock burst during stope mining with interval coal pillar in one-sided mining space. *J. Min. Saf. Eng.* **2020**, *37*, 1213–1221.

23.   Xu, X.; He, F.; Li, X.; Lyu, K.; He, C.; Li, L. Roadway impact mechanism and optimization design under coal pillar disturbance in large mining height working face. *J. Min. Saf. Eng.* **2021**, *38*, 547–555+564.

24.   Zhang, S.; Wang, X.; Fan, G.; Zhang, D.; Cui, J. Pillar size optimization design of isolated island panel gob-side entry driving in deep inclined coal seam-case study of Pingmei No. 6 coal seam. *J. Geophys. Eng.* **2018**, *15*, 816–828. [CrossRef]

25.   Yang, K.; Gou, P. Research on Reasonable Width of Coal Pillars in High Strength Mining Roadway in Wantugou Mine. *Geotech. Geol. Eng.* **2021**, *39*, 2065–2073. [CrossRef]

26.   Li, X.; Zhao, Y.; He, W.; Li, L.; He, F. Study on Coal Pillar Width and Surrounding Rock Control of Gob-Side Entry in Extra-thick Coal Seam. *Geotech. Geol. Eng.* **2020**, *38*, 6855–6868. [CrossRef]

27.   Zhou, K.; Dou, L.; Gong, S.; Chai, Y.; Li, J.; Ma, X.; Song, S. Mechanical behavior of sandstones under water rock interactions. *Geomech. Eng.* **2022**, *29*, 627–643.

28.   Zhao, S.K. A comparative analysis of deep hole roof pre-blasting and directional hydraulic fracture for rockburst control. *J. Min. Saf. Eng.* **2021**, *38*, 706–719.

29.   Gao, X.P. Research on Layout Mode of Small Panel and Large Coal Pillar for Rock Burst Prevention and Control under Huge Thick Key Strata. Master's Thesis, China University of Mining and Technology, Xuzhou, China, 2022. (In Chinese)

30.   Dou, L.M.; Lu, A.L.; Cao, J.R.; Bai, J.Z.; Liu, J.J.; Ma, H.J. Study on stress energy evolution law of irregular coal pillar in double coal seams and anti-scouring technology. *J. Coal Sci. Technol.* **2021**, *42*, 1–9. (In Chinese)

31.   Lu, C.-P.; Liu, G.-J.; Liu, Y.; Zhang, N.; Xue, J.-H.; Zhang, L. Microseismic multi-parameter characteristics of rockburst hazard induced by hard roof fall and high stress concentration. *Int. J. Rock Mech. Min. Sci.* **2015**, *76*, 18–32. [CrossRef]

32.   Yu, Q.; Zhao, D.C.; Xia, Y.J.; Jin, S.J.; Zheng, J.; Meng, Q.K.; Mu, C.Q.; Zhao, J.C. Multivariate Early Warning Method for Rockburst Monitoring Based on Microseismic Activity Characteristics. *Front. Earth Sci.* **2022**, *10*, 837333. [CrossRef]